ACS APPLIED MATERIALS & INTERFACES

Research Article

www.acsami.org

Hyaluronic Acid-Decorated Graphene Oxide Nanohybrids as Nanocarriers for Targeted and pH-Responsive Anticancer Drug Delivery

Erqun Song,*[,†] Weiye Han,[†] Cheng Li,[†] Dan Cheng,[†] Lingrui Li,[†] Lichao Liu,[†] Guizhi Zhu,[‡] Yang Song,[†] and Weihong Tan*[,‡]

[†]Key Laboratory of Luminescence and Real-Time Analytical Chemistry (Southwest University); Ministry of Education, College of Pharmaceutical Sciences, Southwest University, Chongqing, 400715, People's Republic of China

[‡]Center for Research at Bio/Nano Interface, Department of Chemistry and Department of Physiology and Functional Genomics, Shands Cancer Center, UF Genetics Institute and McKnight Brain Institute, University of Florida, Gainesville, Florida 32261-7200, United States

Supporting Information

ABSTRACT: A novel nanohybrid of hyaluronic acid (HA)-decorated graphene oxide (GO) was fabricated as a targeted and pH-responsive drug delivery system for controlling the release of anticancer drug doxorubicin (DOX) for tumor therapy. For the preparation, DOX was first loaded onto GO nanocarriers via $\pi-\pi$ stacking and hydrogen-bonding interactions, and then it was decorated with HA to produce HA−GO−DOX nanohybrids via H-bonding interactions. In this strategy, HA served as both a targeting moiety and a hydrophilic group, making the as-prepared nanohybrids targeting, stable, and disperse. A high loading efficiency (42.9%) of DOX on the nanohybrids was also obtained. Cumulative DOX release from HA−GO−DOX was faster in pH 5.3 phosphate-buffered saline solution than that in pH 7.4, providing the basis for pH-response DOX release in the slightly acidic environment of tumor cells, while the much-slower DOX release from HA−GO−DOX than DOX showed the sustained drug-release capability of the nanohybrids. Fluorescent images of cellular uptake and cell viability analysis studies illustrated that these HA−GO−DOX nanohybrids significantly enhanced DOX accumulation in HA-targeted HepG2 cancer cells compared to HA-nontargeted RBMEC cells and subsequently induced selective cytotoxicity to HepG2 cells. In vivo antitumor efficiency of HA−GO−DOX nanohybrids showed obviously enhanced tumor inhibition rate for H22 hepatic cancer cell-bearing mice compared with free DOX and the GO−DOX formulation. These studies suggest that the HA−GO−DOX nanohybrids have potential clinical applications for anticancer drug delivery.

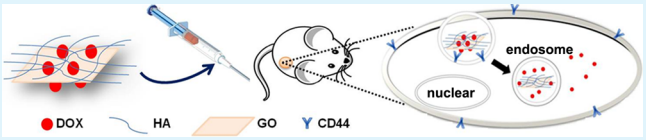

KEYWORDS: *graphene oxide, hyaluronic acid, targeted, drug delivery, cancer, nanocarrier*

1. INTRODUCTION

While chemotherapy is commonly used in cancer therapy, the classic chemotherapeutic agents lack specificity for cancer cells, resulting in high toxicity in normal tissues and low therapeutic efficacy.[1] To overcome this obstacle, considerable efforts have been made to develop targeted delivery systems of anticancer drugs,[2,3] aiming to deliver chemotherapeutic drugs specifically to, or around, cancerous tissues. Two forms of targeted strategies for cancer therapy have thus far been developed: passive and active targeted therapy. The passive strategy takes advantage of the differences in microenvironment between cancerous and normal tissues to improve drug availability by using liposome and nanoparticles as drug carriers based on enhanced permeation and retention (EPR) effects.[2] Active targeting strategies take advantage of overexpression of receptors on cancer cells. Thus, nanoparticles bearing targeting moieties, such as antibodies,[4,5] peptides,[6,7] and other ligands,[8,9] are able to recognize and bind to tumor cells through the specific interactions between targeting moieties and receptors. Therefore, these targetable nanoparticles can serve as nanocarriers for targeted delivery of anticancer drugs.

In recent years, graphene oxide (GO), a new two-dimensional nanoscale material with a single carbon layer,[10] has attracted tremendous attention for its application in anticancer drug loading and delivery, owing to its larger surface area and loading capacity of aromatic molecules via $\pi-\pi$ stacking and hydrogen-bonding interactions.[11−18] However, although GO is monodisperse in pure water, it tends to aggregate in solutions with high concentrations of salts or proteins, such as cell culture medium and serum.[19] To improve the stability and biocompatibility of GO in aqueous phase, hydrophilic groups, such as poly(ethylene glycol) (PEG),[19−21] sulfonic acid groups,[22,23] and polysaccharides,[24] have been grafted onto GO, thus making it more promising as a drug carrier.[25] Furthermore, GO-functionalized specific recognition

Received: July 17, 2013
Accepted: July 7, 2014
Published: July 7, 2014

moieties were investigated as drug nanocarriers for active targeted drug delivery.[20,22] To this end, tumor-recognition moieties, including folic acid (FA), which is a target ligand that selectively binds with FA receptor overexpressed on tumor cells,[22,26] peptides,[27] and antibodies,[20] were conjugated to GO by covalent bonding.[19,20] However, among these targeting moieties, FA is economical, but poorly water-soluble, peptides have limited target cell types, and antibodies have high selectivity, but with the shortcomings of immunogenicity and high cost.

Hyaluronic acid (HA), a linear macromolecule composed of alternating D-glucuronic acid and *N*-acetyl-D-glucosamine, possesses specific recognition capability to transmembrane glycoprotein CD44, which is overexpressed on surfaces of various tumor cells.[28−32] Owing to its outstanding biocompatibility, biodegradability, and specific targeting ability to cancer cells, HA has been extensively investigated for its biomedical and pharmaceutical applications.[32] In particular, HA has been conjugated with drugs or onto various nanoparticles for targeted delivery of antitumor drugs, including paclitaxel[33,34] and doxorubicin (DOX).[35,36] Moreover, compared to other counterparts, such as FA, peptides, or antibodies, HA has better water-solubility and stability, and it is more economical and ubiquitous.

In the present study, an HA−GO−DOX nanohybrid was constructed by conjugating GO with HA via H-bond interaction for targeted delivery of DOX to induce selective cytotoxicity in target cancer cells. In this HA−GO−DOX nanohybrid, DOX is a broad-spectrum anticancer agent commonly used to treat many solid tumors; GO is used as a potential drug carrier that can deliver drugs to tumor cells as described previously;[16,22] HA modified with adipic acid dihydrazide (ADH) functions as both a targeting moiety and a hydrophilic moiety, and provides the pendant hydrazido group for the binding with GO[15] and better coupling and cross-linking ability, tolerance under neutral pH, and resistance to hyaluronidase.[37−39] The construction of HA−GO via H-bonding between the amine group of HA−ADH and epoxy groups in GO[15] could avoid complex covalent modification, which made the whole preparation process easier than that reported in previous studies.[18,40,41] The HA−GO−DOX nanohybrids showed high stability, dispersibility, high drug loading efficiency, and biocompatibility, and they were capable of pH response and sustained drug release. Intracellular drug uptake from HA−GO−DOX was further revealed using fluorescent imaging, and the in vitro selective cytotoxicity induced in target tumor cells compared to control cells was demonstrated using cell viability analysis. Finally, solid tumor inhibition efficacy of HA−GO−DOX nanohybrids compared with free DOX and GO−DOX formulation in vivo was investigated by using an H22 hepatic cancer cells-bearing mouse model. It could be expected that the HA−GO−DOX nanohybrids would have potential clinical applications for cancer therapy.

2. EXPERIMENTAL SECTION

2.1. Materials. Hyaluronic acid (∼3.5 kDa) was purchased from Shandong Dongchen Bioengineering Co., Ltd. (Shandong, China). Fuorescein hyaluronic acid (HA−FITC) was purchased from Sigma-Aldrich. Adipic acid dihydrazide (ADH) and 1-ethyl-3-[3-(dimethylamino)-propyl]carbodiimide (EDC) were purchased from Aladdin Reagent Database, Inc. Doxorubicin hydrochloride (DOX) was purchased from Dalian Meilun Biology Technology Co., Ltd. (Dalian, China). Natural graphite (325 mesh) was purchased from Nanjing Xianfeng Nano Materials Technology Co., Ltd. (Nanjing, China), and 3-(4,5-dimethylthiazol-2-yl)-2,5-diphenyl-tetrazolium bromide (MTT) was purchased from Sigma-Aldrich, Inc. (Shanghai, China). Dialysis bags (cutoff 8000−14 000) was bought from Dingguo Biotechnology Co. (Beijing, China). All other chemicals were of the highest grade commercially available without further purification.

2.2. Synthesis of GO. GO was synthesized from natural graphite by the Hummer method with minor modification.[14,42] In brief, graphite (1.0 g) was mixed with 46 mL of concentrated H_2SO_4 (98%, 46 mL) at 0 °C and was stirred for 10 min, followed by adding $KMnO_4$ (6.0 g) and stirring at 35 °C for 6 h. Subsequently, distilled water (80 mL) was added to the mixture, drop by drop, under intense stirring. The whole mixture was quickly heated to 80 °C and stirred for another 30 min at this temperature. Afterward, distilled water (200 mL) and H_2O_2 solution (30%, 6 mL) were added, in turn, until the color of the mixture changed to yellow. The resultant suspension was washed by distilled water and centrifuged (12 000 rpm for 5 min) repeatedly until the pH value of suspension reached ∼5.0 and no SO_4^{2-} appeared when analyzed using $BaCl_2$. Finally, suspensions were lyophilized.

2.3. Loading of GO with DOX. DOX and GO (with a constant final concentration of 1 mg/mL) were added to distilled water (pH 7). The mixture was stirred under darkness at room temperature for 24 h. Then, the mixture was centrifuged at 12 000 rpm for 5 min and washed with distilled water. Repeated centrifugation was performed until the supernatant was colorless. The precipitation, GO−DOX complex, was collected and freeze-dried.

2.4. Preparation of HA−GO−DOX Nanohybrids. HA is sensitive to strong acid, alkali, free radicals, and hyaluronidase.[43] To overcome this limitation, HA needs to be modified. To accomplish this, we modified HA with ADH according to a previous study.[39] Synthesis details and ^{1}H NMR characterization was shown in Supporting Information. Coating GO−DOX with HA−ADH was accomplished by adding GO−DOX (3 mg) and HA−ADH (6 mg) in phosphate-buffered saline (PBS) (pH 7.4, 6 mL) under stirring at room temperature, keeping the mixture in the dark for 24 h. Afterward, the mixture was centrifuged (12 000 rpm for 5 min) and washed three times to collect HA−GO−DOX. The loading efficiency of DOX was determined as follows. Supernatant was collected to measure unloaded DOX concentration using a standard DOX concentration curve obtained by UV−vis spectrophotometry from DOX solutions with different concentration at the wavelength of 480 nm. The drug loading efficiency (DLE) and entrapment efficiency (EE) of HA−GO−DOX were presented by eq 1 and 2:[44]

$$\mathrm{DLE} = W_{\mathrm{DOX}}/W_{\mathrm{nanohyrid}} \times 100\% \quad (1)$$

$$\mathrm{EE} = W_{\mathrm{DOX}}/W'_{\mathrm{DOX}} \times 100\% \quad (2)$$

where W_{DOX} is the weight of DOX in HA−GO−DOX, $W_{\mathrm{nanohyrid}}$ is the weight of nanohyrid, and W'_{DOX} is the initial weight of DOX added.

2.5. Characterization of GO, GO−DOX, and HA−GO−DOX. GO, GO−DOX, and HA−GO−DOX were characterized by UV−vis spectrophotometry (UV2450, SHIMADZU), fluorospectrophotometry (F-7000, HITACHI), atomic force microscopy (AFM) (Multi-Mode 8, VEECO), Malvern Zetasizer 3000 HS, and Fourier transform infrared (FTIR) (Spectrum-GX, PerkinElmer).

2.6. In Vitro Drug Release. Release of DOX from HA−GO−DOX was achieved using the dialysis method. HA−GO−DOX was dispersed in PBS (2.5 mL) at pH 5.3 (endosomal pH in cancer cells) and pH 7.4 (physiological pH) and was placed in a dialysis bag, which was immersed in homologous PBS (50 mL) under a certain stirring rate at 37 °C. At selected time intervals (1, 2, 3, 4, 5, 6, 7, 8, 9, 10, 11, 12, 24, 36, 48, 72, 96, and 120 h), PBS (2.5 mL) outside the dialysis bag was taken out for UV absorption measurement at a wavelength of 480 nm, and an equal volume of blank PBS was added. Concentration of DOX released into PBS was calculated using a standard DOX concentration curve. This method is also applicable to GO−DOX, using free DOX as control. All experiments were carried out in triplicate. Cumulative DOX release (%) was obtained by eq 3 below:[44]

Scheme 1. Schematic Illustrating the Preparation of HA−GO−DOX Nanohybrid

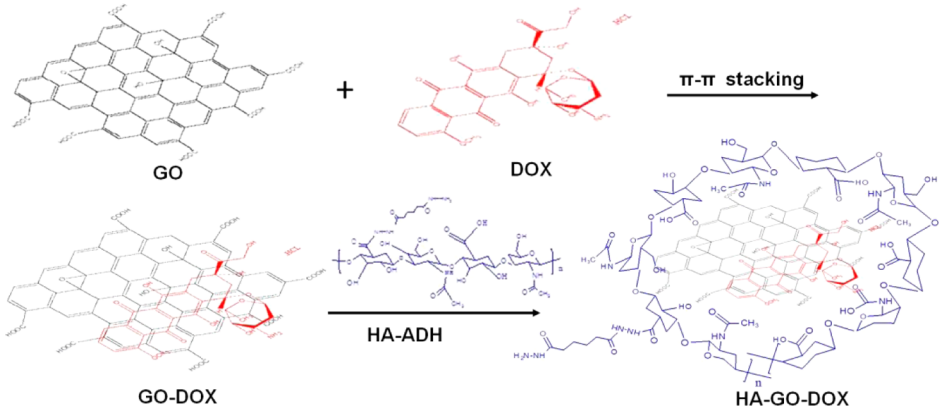

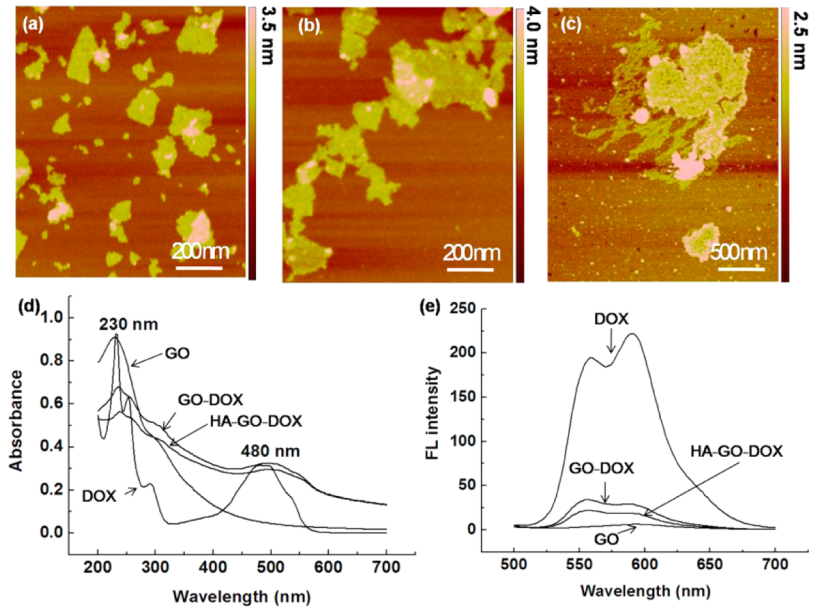

Figure 1. AFM images of GO (a), GO−DOX (b), and HA−GO−DOX (c); UV−vis (d) and fluorescence (at 480 nm excitation) spectra (e) of DOX, GO, GO−DOX, and HA−GO−DOX.

$$Er = \frac{Ve\sum_{i=1}^{n-1} Ci + VoCn}{m} \quad (3)$$

where *Er* is the cumulative DOX release (%); *Ve* is the volume which was taken out (2.5 mL); *Ci* is the concentration at time *i* ($i = n - 1$), μg/mL; *Vo* is the total volume of PBS outside the dialysis bag (50 mL); *Cn* is the concentration at the selected time, μg/mL; and *m* is the total milligram amount of DOX in HA−GO−DOX.

2.7. Cell Culture. Human hepatocellular carcinoma cells (HepG2) were cultured in RPMI 1640 medium (Gibco, Invitrogen Co., USA) with 10% fetal bovine serum (HyClone, USA) and antibiotics (100 U/mL penicillin, 100 μg/mL streptomycin) at 37 °C and 5% CO_2. Rat brain microvascular endothelial cells (RBMEC) were cultured in high glucose-containing Dulbecco's modified Eagle's medium (DMEM) medium (Gibco, Invitrogen Co., USA) with 20% fetal bovine serum (HyClone, USA) and antibiotics (100 U/mL penicillin, 100 μg/mL streptomycin) at 37 °C and 5% CO_2.

2.8. In Vitro Cellular Uptake of HA−GO−DOX by HepG2 and RBMEC Cells. To investigate selective uptake of HA−GO−DOX, HepG2 and RBMEC cells were used. HepG2 cells have overexpression of CD44 receptor, while RBMEC cells have no expression of CD44 receptor. Cells seeded into 6-well plates at 1×10^5 cells/well with culture medium (2 mL) were treated with free DOX, GO−DOX, and HA−GO−DOX at DOX concentration of 5 μg/mL, followed by incubation at 37 °C with a humidified atmosphere containing 5% CO_2 for 3 h. After that, culture media were abandoned, and the cells were washed with PBS (0.01 M, pH 7.4) three times. Fluorescence images of cells were captured with a fluorescence microscope (Olympus IX71). For dose- and time-dependent study, HepG2 cells were treated with free DOX, GO−DOX, and HA−GO−DOX at the DOX concentration of 0.5 μg/mL, 1 μg/mL, and 5 μg/mL, followed by incubation at 37 °C in a humidified atmosphere containing 5% CO_2. After 0.5, 3, and 6 h, the cells were treated using the same method mentioned above.

2.9. In Vitro Cytotoxicity of HA−GO−DOX against HepG2 and RBMEC Cells. To investigate the cytotoxicity of the designed nanohybrid toward tumor cells, an MTT assay was performed. Cells were seeded in culture medium (100 μL) on 96-well plates at a density of 1×10^4 cells per well for 24 h. Cells were incubated with HA−GO, free DOX, GO−DOX and HA−GO−DOX, respectively, for a further 24 h. Then culture medium was removed, and fresh medium containing 3-(4,5-dimethylthiazol-2-yl)-2,5-diphenyltetrazolium bromide (MTT) (final concentration of 0.5 mg/mL) was added. Cells were incubated for another 4 h. Afterward, supernatant was removed, dimethyl sulfoxide (DMSO) (100 μL) was added in each well, and plates were shaken for 15 min. Absorbance of solution of each well was measured using a microplate reader at the wavelength of 570 nm to determine the optical density (OD) value. The MTT assay was performed three times. Relative cellular viability was calculated based on eq 4:[44]

$$\text{relative cellular viability} = \mathrm{OD}_{\text{sample}}/\mathrm{OD}_{\text{control}} \quad (4)$$

where $\mathrm{OD}_{\text{sample}}$ is obtained from cells incubated with DOX, GO−DOX, HA−GO−DOX, or HA−GO, and $\mathrm{OD}_{\text{control}}$ is obtained from cells incubated without the material above.

2.10. In Vivo Antitumor Efficiency of HA−GO−DOX. The healthy male Kunming (KM) mice (Warrant No. SCXK(Yu)-2014−001; age = six weeks; body weight = 18−22 g) were obtained from Chongqing Medical University (Chongqing, China). All animals received care in compliance with the guidelines outlined in the Guide for the Care and Use of Laboratory Animals, and all procedures were approved by the Animal Care and Use Committee.

The in vivo study was performed according to a previous study with some modifications.[45] In brief, the tumor-bearing mouse model was first obtained by implantation of H22 hepatic cancer cells (1×10^7) in the right flank of each mouse. Then the tumor-bearing mice (n = 70) were randomly and equally divided into seven groups on the seventh day of postsubcutaneous. The mice in the control group were treated with physiological saline (PS), and the other six group mice were treated with free DOX, GO−DOX, or HA−GO−DOX, respectively, through the tail vein at a dose of 4 mg kg^{-1} or 6 mg kg^{-1} (on a DOX·HCl basis) on days 0, 3, 7, and 10. On the 12th day of post-tumor implantation, each group of mice was sacrificed, and the tumors were completely excised, followed by weighting.

3. RESULTS AND DISCUSSION

3.1. Characterization of HA−GO−DOX Nanohybrids. In this drug delivery system, GO was used as a drug carrier, DOX was used as a model drug, and HA was used as both targeting and hydrophilic moieties. The preparation of the nanosized HA−GO−DOX complexes is shown in Scheme 1.

Water-soluble GO was synthesized by oxidizing graphite using a modified Hummer method.[21] Sonication treatment of GO brings it into nanosized material with a thickness of less than 2.0 nm and 10−200 nm in lateral width, as verified by AFM characterization (Figure 1a), suggesting a single or two-layer sheet, according to a previous report.[46,47]

We next studied the loading of DOX onto GO, using UV−vis spectrometry. GO has the characteristic peak at 230 nm, and DOX shows strong absorbances at 232, 252, 290, and 480 nm.

As shown in Figure 1d, the two main absorption peaks at 230 and 480 nm of GO−DOX correspond to the characteristic peaks of GO and DOX, respectively. Thus, the presence of characteristic DOX absorption peak clearly indicated the successful loading of DOX onto GO. With 480 nm excitation, the fluorescence spectrum of free DOX displayed a peak at 590 nm, as shown in Figure 1e. However, GO−DOX with the equivalent DOX concentration exhibited significant fluorescent quenching at the same excitation wavelength based on the energy transfer from DOX to GO, which resulted from the strong $\pi-\pi$ stacking interaction between GO and DOX.[48] This fluorescence quenching also confirmed successful loading of DOX onto GO. The AFM image of GO−DOX complex (Figure 1b) shows a slight increase of the thickness compared with free GO as a result of DOX loading.

GO uniformly dispersed in water, but it tended to aggregate upon DOX loading, most likely from the screening of electrostatic charges.[19] In our study, the linear hydrophilic macromolecular HA not only functions in a manner similar to PEG to increase the stability and solubility of GO, but it can also serve as an active targeting moiety to recognize CD44 receptor. As described above, before grafting of HA onto GO−DOX, it was modified with ADH for better biocompatibility. This modification was proved by ^{1}H NMR according to the literature.[37] In our study, the degree of ADH modification was ~15%, as determined by integration of the linker peaks (4H) against the methyl peaks (δ = 1.95 ppm) of the acetamido moiety of the *N*-acetyl-D-glucosamine residue of HA (Supporting Information, Figure S1), which will not affect the receptor-mediated endocytosis of HA.[49] The modified HA was then attached to GO−DOX via H-bonding between the amine group of HA−ADH and epoxy groups in GO,[15] resulting in the HA−GO−DOX nanohybrid.

Compared to GO−DOX, Figure 1d,e shows that HA−GO−DOX has similar UV−vis absorbance and fluorescence signals, except a slight decrease of the absorbance at 230 and 480 nm and the fluorescence at 590 nm, most likely from the coating of HA−ADH. AFM images (Figure 1c) illustrate successful coating of HA onto the GO surface. And the hydrodynamic size distribution of HA−GO−DOX nanohybrids was studied by dynamic light scattering (DLS) method (see Supporting Information, Figure S2).The FTIR spectra were further examined to determine the formation of HA−GO−DOX. As shown in Figure 2a, the peaks at 1114 and 817 cm^{-1} in the FTIR spectrum of DOX were from the stretching bands of C−O−CH_3, while the peaks shown at 871 and 764 cm^{-1} belong to the wagging of $-NH_2$ and deformation bonds of N−H, respectively. The characteristic peaks of GO at 1730 and 1632 cm^{-1} were from the stretching vibration of C═O and deformation of −OH. Figure 2c displays the FTIR spectra of GO−DOX. Compared with DOX and GO shown in Figure 2a,b, there were peaks at 1118 and 814 cm^{-1} (corresponding to

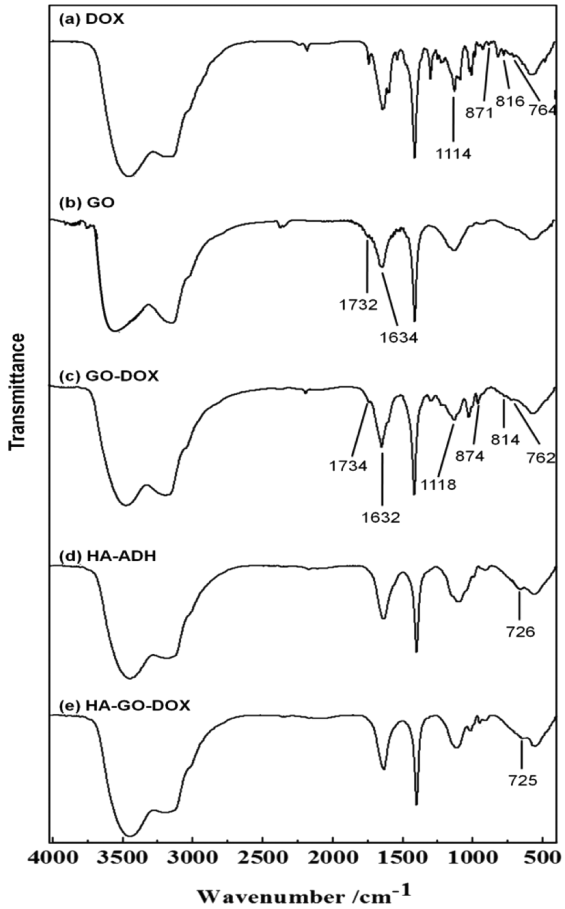

Figure 2. FTIR spectra of DOX (a), GO (b), GO−DOX (c), HA−ADH (d), and HA−GO−DOX (e).

stretching bands of C−O−CH_3 of DOX) and at 874 and 762 cm^{-1} (corresponding to the primary amine NH_2 wag and N−H deformation bonds from DOX), in addition to the characteristic peaks at 1733 and 1632 cm^{-1} belonging to GO. These data confirm the successful loading of DOX onto GO. The FTIR spectrum of HA−GO−DOX is shown in Figure 2e. The characteristic peak at 726 cm^{-1} corresponds to the bending vibration of $(CH_2)_4$ of ADH in HA−ADH, as shown in Figure 2d. An additional peak at 874 cm^{-1} resulted from the wagging of $-NH_2$ of DOX, which shows that GO−DOX was successfully encapsulated by HA−ADH. The DLE_{DOX} of HA−GO−DOX reached 42.9%, and EE_{DOX} of HA−GO−DOX reached 69.5%, which is relatively higher than many other drug carriers, such as polymer nanoparticles.[41,42] The effect of HA density on the performance of HA−GO−DOX nanohybrids (stability, DOX release rate, binding with HepG2 cells, and cell viability) was studied (Supporting Information, Figure S3), and the HA−GO−DOX nanohybrids with HA density of 0.591 mg HA/mg HA−GO−DOX was chosen for further study.

3.2. Stability of HA−GO−DOX Nanohybrids. Stability of a drug-carrier complex is critical for the application of a drug delivery system. In this work, HA was employed to couple with GO−DOX to produce the HA−GO−DOX nanohybrid with improved stability compared to unmodified GO, which tends to aggregate in complex medium environment. Figure 3a shows

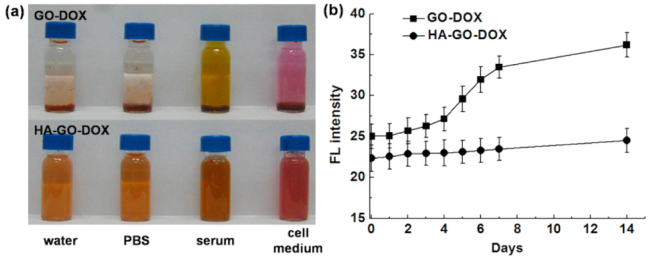

Figure 3. (a) Photos of HA−GO−DOX and GO−DOX in different solutions. (b) Fluorescence intensities of HA−GO−DOX and GO−DOX in water vs storage time.

that no aggregation occurred for the HA−GO−DOX nanohybrids (100 μg/mL) when dispersed in PBS, cell medium, or serum, while GO−DOX aggregated very quickly. Compared with GO−DOX, this test demonstrated that the resulting HA−GO−DOX nanohybrid exhibited excellent stability in all biological solutions tested, including serum. Moreover, the stability of HA−GO−DOX (10 μg/mL) for storage was investigated by measuring the fluorescence of HA−GO−DOX at different storage time intervals when stored in pure water. Figure 3b shows no obvious change of fluorescence intensities for the HA−GO−DOX nanohybrids after storage in water for two weeks at 4 °C, indicating their good stability for storage. The above-mentioned tests show that the introduction of HA does, indeed, enhance the stability of the whole HA−GO−DOX nanohybrid.

3.3. In Vitro Drug Release of HA−GO−DOX Nanohybrids. We next evaluated whether DOX could be delivered and released from the nanohybrids. Drug release from a carrier depends on different experimental factors, such as pH, carrier materials, particle sizes, and interactions between drug and carriers. Herein, in vitro release behavior of DOX from HA−GO−DOX was first investigated under different pH values. Figure 4a shows DOX release profiles from HA−GO−DOX at 37 °C in phosphate buffer solutions with pH of 7.4 and 5.3, which represent normal physiological pH and acidic environment of tumor cell, respectively. It was found that the cumulative DOX release of HA−GO−DOX reached 40% in pH 5.3 PBS in 24 h, while it achieved less than 20% of DOX release in pH 7.4 PBS, suggesting that an acidic solution facilitated DOX release. It is likely that DOX became more hydrophilic and water-soluble in pH 5.3 buffer, which increased DOX release rate.[22] Figure 4b shows DOX release profiles of free DOX itself, GO−DOX, and HA−GO−DOX at 37 °C in phosphate buffer solutions with pH of 5.3. Compared with free DOX, the release rates of DOX from both GO−DOX and HA−GO−DOX systems were slower in pH 5.3 PBS within 24 h. This could be ascribed to the strong hydrogen-bond and $\pi-\pi$ stacking interactions between DOX and GO. Moreover, compared with GO−DOX, HA−GO−DOX nanohybrids showed a lower release rate of DOX, which is presumably because the HA−ADH conjugate offers a diffusion barrier to retard DOX release after encapsulating GO−DOX.[50] This pH-activated, sustained drug release is expected to facilitate targeted drug release in the acidic environment of tumor cells or in intracellular compartments, such as endosome.

3.4. In Vitro Cellular Uptake of HA−GO−DOX by HepG2 and RBMEC Cells. To study the selective cell uptake of HA−GO−DOX, cell lines HepG2 (target cells, with overexpressed CD44) and RBMEC (nontarget cells, without overexpressed CD44) were employed. Before studying the cellular uptake of HA−GO−DOX by the chosen model cells,

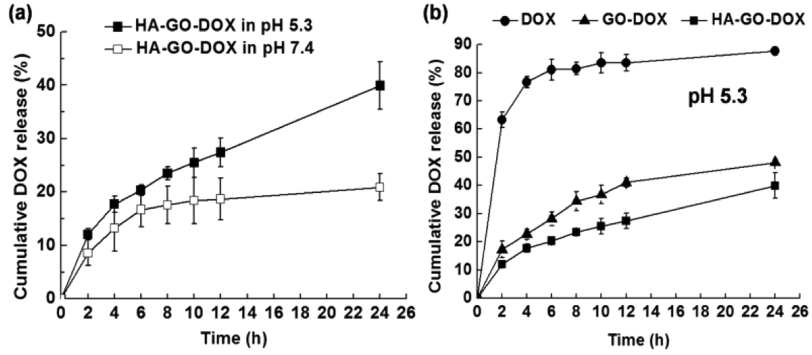

Figure 4. Cumulative DOX release (%) from HA−GO−DOX in PBS with pH of 7.4 and pH 5.3 at 37 °C (a). Cumulative DOX release (%) from DOX, GO−DOX, and HA−GO−DOX in PBS with pH of 5.3 at 37 °C (b). The data points are the average of three experiments. Error bars represent the range over which the values were observed.

the selective binding of HA to HepG2 cells other than RBEMC cells was confirmed by flow cytometry analysis after treating HepG2 cells and RBEMC cells with HA−FITC. Flow cytometry results (Supporting Information, Figure S4) showed that, compared with no FITC fluorescent signal shift of RBEMC cells, the sample of HepG2 cells exhibited distinct FITC fluorescent signal shift after incubating with HA−FITC, demonstrating HA can specifically bind with CD44 overexpressed HepG2 cells but not binding with RBMEC cells.

Cellular uptake of drug was evaluated using fluorescence microscopy after incubation of cells and drugs, or nanohybrids, for 3 h. HepG2 cells treated with HA−GO−DOX showed much stronger fluorescence intensity than cells treated with free DOX or GO−DOX with the same DOX equivalent concentrations, even though the amount of DOX released from HA−GO−DOX (15.4%) was lower than that of free DOX (72.7%) and GO−DOX (20.4%) at 3 h, indicating that endocytosis mediated by CD44 receptor facilitates cellular uptake efficiency. In contrast, in RBMEC cells, the fluorescence signal of the free DOX group was the strongest, while that of the HA−GO−DOX group was the weakest (Figure 5). Since

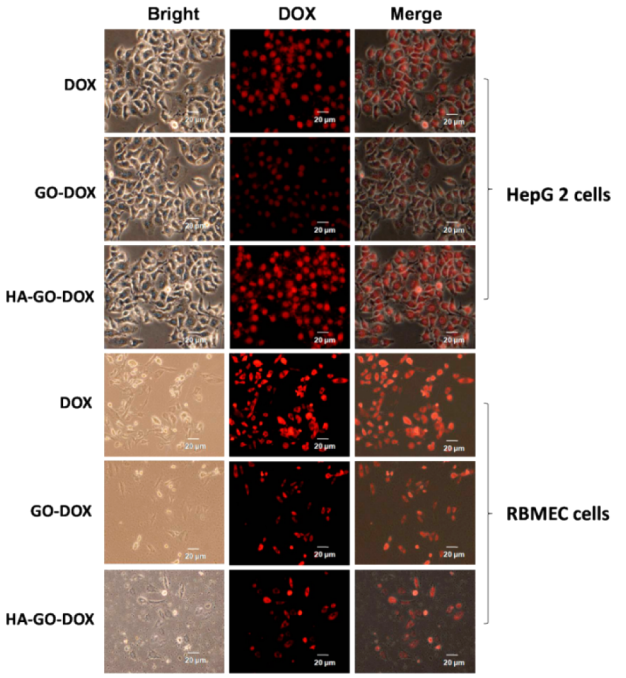

Figure 5. Fluorescent microscopy images showing cellular uptake of DOX, GO−DOX, and HA−GO−DOX by HepG2 and RBMEC cells. The cells were treated with free DOX and HA−GO−DOX (DOX equivalent = 5 μg/mL) for 3 h.

fewer CD44 receptors are present on RBMEC cells, the HA−GO−DOX complex was mainly uptaken through passive means, and the HA−ADH shell had retarded the release of DOX. The selective drug uptake in target cells provides the basis for targeted therapy mediated by HA−GO nanocarriers.

Further study showed that cellular uptake and release of DOX in HepG2 cells was both time- and dose-dependent. At low DOX concentration (0.5 μg/mL) for each sample (free DOX, GO−DOX, and HA−GO−DOX), HepG2 cells incubated with HA−GO−DOX exhibited the strongest fluorescence signals (Supporting Information, Figure S5), even though DOX release rate was the slowest from the HA−GO−DOX nanohybrid (Figure 4). This demonstrated selective uptake of HA−GO−DOX nanohybrid by HepG2 cells based on the HA targeting to CD44 receptor overexpressed on HepG2 cells. Moreover, the fluorescence signals from HepG2 cells were enhanced with the increase of the incubation time for all three groups (DOX, GO−DOX, HA−GO−DOX), which is consistent with the in vitro drug release behavior as shown in Figure 4. However, when the concentration of pure DOX was increased to 5 μg/mL, no obvious difference of the fluorescence signals was observed from HepG2 cells for either free DOX or HA−GO−DOX nanohybrid groups after incubating for 6 h. This might be ascribed to the saturation of DOX for the chosen model cells under our experimental condition, which means that the uptake by HepG2 cells had been exhausted. The weaker fluorescence signal from HepG2 cells incubated with GO−DOX in contrast to the relatively stronger fluorescence signals from either free DOX or HA−GO−DOX can be attributed to the slower release rate of DOX and the lack of a targeting moiety. This experiment, along with the fluorescence images shown in Figure 5, strongly suggests specific uptake of HA−GO−DOX by HepG2 cells, presumably via receptor-mediated endocytosis, and it also suggests that the HA−GO−DOX nanohybrids can effectively deliver drugs to the target tumor cells.

3.5. Cytotoxicity of HA−GO−DOX in HepG2 and RBMEC cells. Having demonstrated the selective targeting of HA−GO−DOX to target HepG2 cells, the selective cytotoxicity effect of HA−GO−DOX nanohybrids was further evaluated using an MTT assay. The cytotoxicity of HA−GO nanocarrier itself was first studied. Figure 6 shows the relative

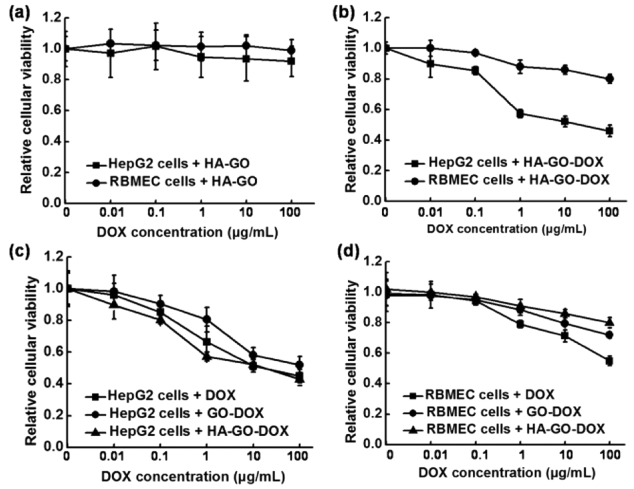

Figure 6. Relative cell viability of HepG2 cells (target cells) and RBMEC cells (control cells) after treatment with HA−GO nanocarrier(a), HA−GO−DOX (b), free DOX (c, d), GO−DOX (c, d) at different concentrations for 24 h.

cellular viability of HepG2 cells and RBMEC cells treated with HA−GO nanocarriers, free DOX, GO−DOX, and HA−GO−DOX, respectively. After 24 h incubation, we found that HA−GO nanocarriers did not induce obvious cytotoxicity to these cells, even at a concentration of 100 μg/mL (Figure 6a), indicating good biocompatibility of this drug carrier under our experimental conditions. The cytotoxicity of free DOX, GO−DOX and HA−GO−DOX was next evaluated (Figure 6b,c,d). Results indicated that HA−GO−DOX presented much more cytotoxicity to HepG2 cells than RBMEC cells (Figure 6b).

Table 1. Effect of HA−GO−DOX on the tumor weight of mice bearing H22 hepatic cancer cell (mean ± SD, n = 10)

group	dose of DOX (mg·kg^{-1})	average tumor weight (g)	inhibition rate (%)
HA−GO−DOX	4	0.1258 ± 0.0592^{a,b,d}	34.45
HA−GO−DOX	6	0.1002 ± 0.0476^{a,b,c}	48.59
GO−DOX	4	0.1582 ± 0.0462^{a}	18.83
GO−DOX	6	0.1325 ± 0.0435^{a,b,d}	32.02
DOX	4	0.1348 ± 0.0440^{a}	30.79
DOX	6	0.1229 ± 0.0581^{a,b,d}	36.92
PS		0.1949 ± 0.0655	

$^{a}p < 0.05$ vs PS group. $^{b}p < 0.05$ vs GO−DOX(4 mg kg^{-1}) group. $^{c}p < 0.05$ vs GO−DOX (6 mg kg^{-1}) group. $^{d}P < 0.05$ vs HA−GO−DOX (6 mg kg^{-1}) group.

Meanwhile, at a lower concentration of DOX equivalent (1 μg/mL), HA−GO−DOX showed a much higher cytotoxicity to HepG2 cells than free DOX and GO−DOX (Figure 6c), even though the release amount of DOX from HA−GO−DOX (39.9%) was lower than that of free DOX (87.7%) and GO−DOX (48.2%) at 24 h. That might be ascribed to more uptake of DOX by HepG2 cells as a consequence of CD44 receptor-mediated endocytosis (Figure 5). In contrast, the cytotoxicity of HA−GO−DOX to RBMEC cells was lower than that of either free DOX or GO−DOX(Figure 6d). These results suggested that, at low DOX dosage of 1 μg/mL, the HA−GO−DOX nanohybrids were much more cytotoxic to target HepG2 tumor cells than either GO−DOX or free DOX, while, at the same time, they were less cytotoxic to normal cells due to the targeted, pH-response, and sustained drug release profiles of HA−GO−DOX nanohybrids. These results suggested that the use of the HA−GO−DOX nanohybrids drug system not only reduces the dosage of DOX with the same cytotoxicity to tumor cells, but also reduces side effects to normal cells, making the HA−GO−DOX nanohybrid potentially promising for clinical targeted cancer therapy.

3.6. In Vivo Anticancer Efficacy of HA−GO−DOX. The antitumor effect of HA−GO−DOX in vivo was evaluated by tumor inhibition rate in a H22 hepatic cancer cells bearing-mouse model. The tumor inhibition rate was calculated by the following eq 5 reported in previous work:[51]

$$\text{Inhibition rate} = (W_{\text{control}} - W_{\text{experimental}})/W_{\text{control}} \times 100\% \quad (5)$$

Where W_{control} and $W_{\text{experimental}}$ are the average tumor weights in the control and experimental group, respectively. The tumor inhibition rate is shown in Table 1. The mean weight of tumor in the treatment groups (DOX, GO−DOX, and HA−GO−DOX) was significantly lower than in the PS group ($P < 0.05$). At the 12 day implantation, the tumor inhibition rates of groups of DOX and GO−DOX with dose of 4 mg kg^{-1} are 30.79% and 18.83% respectively while 36.92% and 32.02% respectively for dose of 6 mg kg^{-1}, which are much lower than the tumor inhibition rate from group of HA−GO−DOX at the same dose (34.45% for 4 mg kg^{-1}, 48.59% for 6 mg kg^{-1}). These results indicate that the HA−GO−DOX inhibited tumor growth much more efficiently than free DOX and GO−DOX formulation under same condition. Comparison between group of HA−GO−DOX (4 mg kg^{-1}) and HA−GO−DOX (6 mg kg^{-1}) showed obvious dose dependence of the tumor inhibition ($p < 0.05$), and the most efficient inhibition of tumor growth was observed in the group of HA−GO−DOX treated at a dose of 6 mg kg^{-1}. The enhanced tumor inhibition rate of the HA−GO−DOX could be attributed to the sustained DOX release in the tumor tissue after nanohybrids accumulation via the receptor-mediated binding with targeted cells.

4. CONCLUSION

In summary, we have developed a novel HA−GO−DOX nanohybrid based on a simple and effective method. The as-prepared nanohybrids possessed excellent physiological stability, high drug loading capacity for DOX (42.9%), the ability of pH response, and sustained release of anticancer drugs. In vitro cellular uptake study and cytotoxicity assays showed that the HA−GO−DOX nanohybrids could specifically deliver DOX to target HepG2 cells, and then efficiently inhibit the proliferation of HepG2 cells, without obvious side effects to control cells, confirming their ability of targeted delivery. The in vivo anticancer efficacy study using an H22 hepatic cancer cell-bearing mouse model demonstrated higher tumor inhibition rate of HA−GO−DOX compared to free DOX and GO−DOX formulation at an equivalent drug dose. Taken together, this work demonstrates an efficient strategy to construct novel HA−GO−DOX nanohybrids, which shows great potential for clinical tumor therapy applications.

■ ASSOCIATED CONTENT

Supporting Information

^{1}H NMR of HA−ADH complex, hydrodynamic size distribution of HA−GO−DOX nanohybrids, the effect of HA density on the performance of HA−GO−DOX nanohybrids (stability, DOX release rate, binding with HepG2 cells, and cell viability), flow cytometry analysis of HA−FITC binding with RBMEC cells and HepG2 cells, and dose and time-dependent study of cellular uptake and release of DOX in HepG2 cells. This material is available free of charge via the Internet at http://pubs.acs.org.

■ AUTHOR INFORMATION

Corresponding Authors

*E-mail: eqsong@swu.edu.cn. Fax: +862368251225. Phone: +862368251225. (E.S.)

*E-mail: tan@chem.ufl.edu. Fax: +01352 3921743. Phone: +01352 3921743. (W.T.)

Notes

The authors declare no competing financial interest.

■ ACKNOWLEDGMENTS

This work was supported by the National Natural Science Foundation of China (21005064, 21035005), Fundamental Research Funds for the Central Universities (XDJK2013B009, XDJK2014A020), the finance from State Key Laboratory of Chemo/Biosensing and Chemometrics, Hunan Univeristy

(2012009), and the Program for Innovative Research Team in University of Chongqing (2013). The authors would like to thank Prof. X. Xu for donating cell lines.

REFERENCES

(1) Arias, J. L. Drug Targeting Strategies in Cancer Treatment: An Overview. *Mini-Rev. Med. Chem.* **2011**, *11*, 1−17.
(2) Mohanty, C.; Das, M.; Kanwar, J. R.; Sahoo, S. K. Receptor Mediated Tumor Targeting: An Emerging Approach for Cancer Therapy. *Curr. Drug Delivery* **2011**, *8*, 45−58.
(3) Platt, V. M.; Szoka, F. C. Anticancer Therapeutics: Targeting Macromolecules and Nanocarriers to Hyaluronan or CD44, A Hyaluronan Receptor. *Mol. Pharmaceutics* **2008**, *5*, 474−486.
(4) Park, J. W.; Kirpotin, D. B.; Hong, K.; Shalaby, R.; Shao, Y.; Nielsen, U. B.; Marks, J. D.; Papahadjopoulos, D.; Benz, C. C. Tumor Targeting Using anti-HER2 Immunoliposomes. *J. Controlled Release* **2001**, *74*, 95−113.
(5) Song, H.; He, R.; Wang, K.; Ruan, J.; Bao, C. C.; Li, N.; Ji, J.; Cui, D. Anti-HIF-1alpha Antibody-Conjugated Pluronic Triblock Copolymers Encapsulated with Paclitaxel for Tumor Targeting Therapy. *Biomaterials* **2010**, *31*, 2302−2312.
(6) Han, L. A.; Huang, R. Q.; Liu, S. H.; Huang, S. X.; Jiang, C. Peptide-Conjugated PAMAM for Targeted Doxorubicin Delivery to Transferrin Receptor Overexpressed Tumors. *Mol. Pharmaceutics* **2010**, *7*, 2156−2165.
(7) Zhang, Z.; Hatta, H.; Tanabe, K.; Nishimoto, S. A New Class of 5-Fluoro-2′-Deoxyuridine Prodrugs Conjugated with a Tumor-Homing Cyclic Peptide CNGRC by Ester Linkers: Synthesis, Reactivity, and Tumor-Cell-Selective Cytotoxicity. *Pharm. Res.* **2005**, *22*, 381−389.
(8) Chen, T.; Shukoor, M. I.; Chen, Y.; Yuan, Q. A.; Zhu, Z.; Zhao, Z. L.; Gulbakan, B.; Tan, W. H. Aptamer-Conjugated Nanomaterials for Bioanalysis and Biotechnology Applications. *Nanoscale* **2011**, *3*, 546−556.
(9) Zhu, G. Z.; Meng, L.; Ye, M.; Yang, L.; Sefah, K.; O'Donoghue, M. B.; Chen, Y.; Xiong, X. L.; Huang, J.; Song, E. Q.; Tan, W. H. Self-Assembled Aptamer-Based Drug Carriers for Bispecific Cytotoxicity to Cancer Cells. *Chem.—Asian J.* **2012**, *7*, 1630−1636.
(10) Novoselov, K. S.; Geim, A. K.; Morozov, S. V.; Jiang, D.; Zhang, Y.; Dubonos, S. V.; Grigorieva, I. V.; Firsov, A. A. Electric Field Effect in Atomically Thin Carbon Films. *Science* **2004**, *306*, 666−669.
(11) Geim, A. K.; Novoselov, K. S. The Rise of Graphene. *Nat. Mater.* **2007**, *6*, 183−191.
(12) Kim, K. S.; Zhao, Y.; Jang, H.; Lee, S. Y.; Kim, J. M.; Kim, K. S.; Ahn, J. H.; Kim, P.; Choi, J. Y.; Hong, B. H. Large-Scale Pattern Growth of Graphene Films for Stretchable Transparent Electrodes. *Nature* **2009**, *457*, 706−710.
(13) Service, R. F. Carbon Sheets An Atom Thick Give Rise to Graphene Dreams. *Science* **2009**, *324*, 875−877.
(14) Zhou, X. F.; Liu, Z. P. A Scalable, Solution-Phase Processing Route to Graphene Oxide and Graphene Ultralarge Sheets. *Chem. Commun.* **2010**, *46*, 2611−2613.
(15) Pandey, H.; Parashar, V.; Parashar, R.; Prakash, R.; Ramteke, P. W. Controlled Drug Release Characteristics and Enhanced Antibacterial Effect of Graphene Nanosheets Containing Gentamicin Sulfate. *Nanoscale* **2011**, *3*, 4104−4108.
(16) Miao, W.; Shim, G.; Lee, S.; Choe, Y. S.; Oh, Y. K. Safety and Tumor Tissue Accumulation of Pegylated Graphene Oxide Nanosheets for Co-delivery of Anticancer Drug and Photosensitizer. *Biomaterials* **2013**, *34*, 3402−3410.
(17) Xu, C.; Yang, D. R.; Mei, L.; Li, Q. H.; Zhu, H. Z.; Wang, T. H. Targeting Chemophotothermal Therapy of Hepatoma by Gold Nanorods/Graphene Oxide Core/Shell Nanocomposites. *ACS Appl. Mater. Interfaces* **2013**, *5*, 12911−12920.
(18) Wu, H. X.; Shi, H. L.; Wang, Y. P.; Jia, X. Q.; Tang, C. Z.; Zhang, J. M.; Yang, S. P. Hyaluronic Acid Conjugated Graphene Oxide for Targeted Drug Delivery. *Carbon* **2014**, *69*, 379−389.
(19) Liu, Z.; Robinson, J. T.; Sun, X. M.; Dai, H. J. PEGylated Nanographene Oxide for Delivery of Water-Insoluble Cancer Drugs. *J. Am. Chem. Soc.* **2008**, *130*, 10876−10877.
(20) Sun, X. M.; Liu, Z.; Welsher, K.; Robinson, J. T.; Goodwin, A.; Zaric, S.; Dai, H. J. Nano-graphene Oxide for Cellular Imaging and Drug Delivery. *Nano Res.* **2008**, *1*, 203−212.
(21) Kim, H.; Kim, W. J. Photothermally Controlled Gene Delivery by Reduced Graphene Oxide-Polyethylenimine Nanocomposite. *Small* **2014**, *10*, 117−126.
(22) Zhang, L. M.; Xia, J. G.; Zhao, Q. H.; Liu, L. W.; Zhang, Z. J. Functional Graphene Oxide as a Nanocarrier for Controlled Loading and Targeted Delivery of Mixed Anticancer Drugs. *Small* **2010**, *6*, 537−544.
(23) Si, Y.; Samulski, E. T. Synthesis of Water Soluble Graphene. *Nano Lett.* **2008**, *8*, 1679−1682.
(24) Bao, H. Q.; Pan, Y. Z.; Ping, Y.; Sahoo, N. G.; Wu, T. F.; Li, L.; Li, J.; Gan, L. H. Chitosan-Functionalized Graphene Oxide as A Nanocarrier for Drug and Gene Delivery. *Small* **2011**, *7*, 1569−1578.
(25) Naahidi, S.; Jafari, M.; Edalat, F.; Raymond, K.; Khademhosseini, A.; Chen, P. Biocompatibility of Engineered Nanoparticles for Drug Delivery. *J. Controlled Release* **2013**, *166*, 182−194.
(26) Yang, Y.; Zhang, Y. M.; Chen, Y.; Zhao, D.; Chen, J. T.; Liu, Y. Construction of A Graphene Oxide Based Noncovalent Multiple Nanosupramolecular Assembly as A Scaffold for Drug Delivery. *Chem.—Eur. J.* **2012**, *18*, 4208−4215.
(27) Robinson, J. T.; Tabakman, S. M.; Liang, Y. Y.; Wang, H. L.; Casalongue, H. S.; Vinh, D.; Dai, H. J. Ultrasmall Reduced Graphene Oxide with High Near-infrared Absorbance for Photothermal Therapy. *J. Am. Chem. Soc.* **2011**, *133*, 6825−6831.
(28) Yadav, A. K.; Mishra, P.; Agrawal, G. P. An Insight on Hyaluronic Acid in Drug Targeting and Drug Delivery. *J. Drug Targeting.* **2008**, *16*, 91−107.
(29) Slevin, M.; Krupinski, J.; Gaffney, J.; Matou, S.; West, D.; Delisser, H.; Savani, R. C.; Kumar, S. Hyaluronan-Mediated Angiogenesis in Vascular Disease: Uncovering RHAMM and CD44 Receptor Signaling Pathways. *Matrix Biol.* **2007**, *26*, 58−68.
(30) Liu, Y. H.; Sun, J.; Cao, W.; Yang, J. H.; Lian, H.; Li, X.; Sun, Y. H.; Wang, Y. J.; Wang, S. L.; He, Z. G. Dual Targeting Folate-Conjugated Hyaluronic Acid Polymeric Micelles for Paclitaxel Delivery. *Int. J. Pharm.* **2011**, *421*, 160−169.
(31) Cho, H. J.; Yoon, H. Y.; Koo, H.; Ko, S. H.; Shim, J. S.; Lee, J. H.; Kim, K.; Kwon, I. C.; Kim, D. D. Self-assembled Nanoparticles Based on Hyaluronic Acid-Ceramide (HA−CE) and Pluronic(R) for Tumor-Targeted Delivery of Docetaxel. *Biomaterials* **2011**, *32*, 7181−7190.
(32) Prestwich, G. D. Hyaluronic Acid-based Clinical Biomaterials Derived for Cell and Molecule Delivery in Regenerative Medicine. *J. Controlled Release* **2011**, *155*, 193−199.
(33) Luo, Y.; Ziebell, M. R.; Prestwich, G. D. A Hyaluronic Acid-Taxol Antitumor Bioconjugate Targeted to Cancer Cells. *Biomacromolecules* **2000**, *1*, 208−218.
(34) Song, S. S.; Chen, F.; Qi, H.; Li, F.; Xin, T. G.; Xu, J. W.; Ye, T. T.; Sheng, N. C.; Yang, X. G.; Pan, W. S. Multifunctional Tumor-Targeting Nanocarriers Based on Hyaluronic Acid-Mediated and pH-Sensitive Properties for Efficient Delivery of Docetaxel. *Pharm. Res.* **2014**, *31*, 1032−1045.
(35) Eliaz, R. E.; Szoka, F. C. Liposome-Encapsulated Doxorubicin Targeted to CD44: A Strategy to Kill CD44-overexpressing Tumor Cells. *Cancer Res.* **2001**, *61*, 2592−2601.
(36) Han, M.; Lv, Q.; Tang, X. J.; Hu, Y. L.; Xu, D. H.; Li, F. Z.; Liang, W. Q.; Gao, J. Q. Overcoming Drug Resistance of MCF-7/ADR Cells by Altering Intracellular Distribution of Doxorubicin via MVP Knockdown with A Novel siRNA Polyamidoamine-hyaluronic Acid Complex. *J. Controlled Release* **2012**, *163*, 136−144.
(37) Pouyani, T.; Prestwich, G. D. Functionalized Derivatives of Hyaluronic Acid Oligosaccharides: Drug Carriers and Novel Biomaterials. *Bioconjugate Chem.* **1994**, *5*, 339−347.

(38) Choi, K. Y.; Yoon, H. Y.; Kim, J. H.; Bae, S. M.; Park, R. W.; Kang, Y. M.; Kim, I. S.; Kwon, I. C.; Choi, K.; Jeong, S. Y.; Kim, K.; Park, J. H. Smart Nanocarrier Based on PEGylated Hyaluronic Acid for Cancer Therapy. *ACS Nano* **2011**, *5*, 8591−8599.
(39) Luo, Y.; Prestwich, G. D. Synthesis and Selective Cytotoxicity of a Hyaluronic Acid-Antitumor Bioconjugate. *Bioconjugate Chem.* **1999**, *10*, 755−763.
(40) Choi, K. Y.; Min, K. H.; Na, J. H.; Choi, K.; Kim, K.; Park, J. H.; Kwon, I. C.; Jeong, S. Y. Self-assembled Hyaluronic Acid Nanoparticles as A Potential Drug Carrier for Cancer Therapy: Synthesis, Characterization, and in Vivo Biodistribution. *J. Mater. Chem.* **2009**, *19*, 4102−4107.
(41) Zhou, Q.; Guo, X.; Chen, T.; Zhang, Z.; Shao, S. J.; Luo, C.; Li, J. R.; Zhou, S. B. Target-Specific Cellular Uptake of Folate-Decorated Biodegradable Polymer Micelles. *J. Phys. Chem. B* **2011**, *115*, 12662−12670.
(42) Hummers, W. S.; Offeman, R. E. Preparation of Graphitic Oxide. *J. Am. Chem. Soc.* **1958**, *80*, 1339.
(43) Lapcik, L.; Lapcik, L., Jr.; Smedt, S. De; Demeester, J.; Chabrecek, P. Hyaluronan: Preparation, Structure, Properties, and Applications. *Chem. Rev.* **1998**, *98*, 2663−2684.
(44) Zhang, Y.; Li, J. S.; Lang, M. D.; Tang, X. L.; L, i L.; Shen, X. Z. Folate-Functionalized Nanoparticles for Controlled 5-Fluorouracil Delivery. *J. Colloid Interface Sci.* **2011**, *354*, 202−209.
(45) Li, M. Q.; Song, W. T.; Tang, Z. H.; Lv, S. X.; Lin, L.; Sun, H.; Li, Q. S.; Yang, Y.; Hong, H.; Chen, X. S. Nanoscaled Poly(l-glutamic acid)/Doxorubicin-Amphiphile Complex as pH-responsive Drug Delivery System for Effective Treatment of Nonsmall Cell Lung Cancer. *ACS Appl. Mater. Interfaces* **2013**, *5*, 1781−1792.
(46) Dikin, D. A.; Stankovich, S.; Zimney, E. J.; Piner, R. D.; Dommett, G. H. B.; Evmenenko, G.; Nguyen, S. T.; Ruoff, R. S. Preparation and Characterization of Graphene Oxide Paper. *Nature* **2007**, *448*, 457−460.
(47) Li, X. L.; Wang, X. R.; Zhang, L.; Lee, S. W.; Dai, H. J. Chemically Derived, Ultrasmooth Graphene Nanoribbon Semiconductors. *Science* **2008**, *319*, 1229−1232.
(48) Guo, Z.; Du, F.; Ren, D. M.; Chen, Y. S.; Zheng, J. Y.; Liu, Z. B.; Tian, J. G. Covalently Porphyrin-Functionalized Single-Walled Carbon Nanotubes: A Novel Photoactive and Optical Limiting Donor-Acceptor Nanohybrid. *J. Mater. Chem.* **2006**, *16*, 3021−3030.
(49) Jiang, G.; Park, K.; Kim, J.; Kim, K. S.; Hahn, S. K. Target Specific Intracellular Delivery of siRNA/PEI-HA Complex by Receptor Mediated Endocytosis. *Mol. Pharmaceutics* **2009**, *6*, 727−737.
(50) Depan, D.; Shah, J.; Misra, R. D. K. Controlled Release of Drug from Folate-Decorated and Graphene Mediated Drug Delivery System: Synthesis, Loading Efficiency, and Drug Release Response. *Mater. Sci. Eng., C* **2011**, *31*, 1305−1312.
(51) Tian, Q. E.; Li, H. D.; Yan, M.; Cai, H. L.; Tan, Q. Y.; Zhang, W. Y. Astragalus Polysaccharides Can Regulate Cytokine and P-glycoprotein Expression in H22 Tumor-Bearing Mice. *World J. Gastroenterol.* **2012**, *18*, 7079−7086.